ELSEVIER

Journal of Alloys and Compounds 330–332 (2002) 93–98

Journal of ALLOYS AND COMPOUNDS

www.elsevier.com/locate/jallcom

The initial stage of the hydriding of gadolinium metal at 100°C and sub-ambient pressure

Mordechai Brill[a,*], Itzhak Halevy[a], Giora Kimmel[a], Moshe H. Mintz[a,b], Joseph Bloch[a]

[a]*Nuclear Research Center-Negev, P.O. Box 9001, Beer Sheva 84190, Israel*

[b]*Ben Gurion University of the Negev, Department of Nuclear Engineering, P.O. Box 653, Beer Sheva 84105, Israel*

Abstract

The development of di- and trihydride phases on gadolinium metallic samples during the initial stage of the hydriding reaction at 100°C and under 0.5 atm of hydrogen was studied using combined microscopic examination, X-ray diffraction (XRD), and hydrogen absorption measurements. Samples were exposed to hydrogen for various times and the amount of hydrogen absorbed was measured. The reaction was then stopped and the samples were removed and examined microscopically to determine the degree of hydride development on the samples surfaces. XRD measurements were performed on the partially hydrided samples. The sequential formation of GdH_2 and GdH_3 was identified for the first time. The topochemical development of the hydride phases on gadolinium is discussed, based on the experimental results. It was found that following a short nucleation and growth of the dihydride phase, at a relatively early stage of the hydriding reaction, the trihydride is formed on top of the dihydride growing nuclei, so that when the hydride layer formation on the sample is completed, it is already constructed of both hydrides.

Keywords: Gadolinium; Dihydrides; Trihydrides; X-Ray diffraction; Hydride-forming metals; Rare-earth metals

1. Introduction

Many hydride-forming metals produce at least two hydride phases under appropriate pressure and temperature conditions. Thus, all the rare-earth metals (except Eu) form two types of hydride phases, namely dihydrides and trihydrides [1]. During the hydriding process both hydride phases are likely to appear, even though the final product of the reaction is the trihydride. It is assumed that the dihydride is initially formed, being the precursor for the formation of the trihydride. In fact, there are two reaction processes taking part in parallel, namely, the transformation of the metal into dihydride and that of the dihydride into trihydride. In analyzing the hydriding mechanism, the separation of those two reactions should be considered. Under special experimental conditions such a separation can be obtained from the overall kinetic curve. In titanium, for example, under hydrogen working pressure much higher than the dissociation pressure of the monohydride, but not much higher than that of the dihydride, the difference between the two reactions rates leads to two separate stages clearly distinguished in the overall hydriding kinetic curve [2]. However, this method is limited and cannot be applied in cases for which the working pressure is much higher than the dissociation pressures of both hydrides.

The hydriding of rare-earth metals in their bulk form is a complex topochemical process. On exposure to hydrogen, nuclei of hydride phase are formed under the surface passivation layer (SPL) and grow until the metallic surface is completely covered with hydride [2,3]. The SPL then may be fractured, getting unimportant during the following stages of the hydriding process. The main reaction stage, starting at this point, is the progress of the hydride front into the bulk metallic sample (a 'contracting envelope' mechanism). For metals hydrided under such mechanism, a steady state condition may be achieved during which the two hydride layers are moving simultaneously, retaining their relative thickness and hydrogen concentration gradients [2]. The structure of the composite hydride layer moving into the bulk of the sample during the steady state stage of the reaction is schematically presented in Fig. 1. A rate-limiting step [4] may be located at the gas phase–trihydride interface, (hydrogen molecule chemisorption), Fig. 1a. The rate limiting step can be the hydrogen atom

*Corresponding author.

E-mail address: mbrill@netvision.net.il (M. Brill).

0925-8388/02/$ – see front matter
PII: S0925-8388(01)01520-1

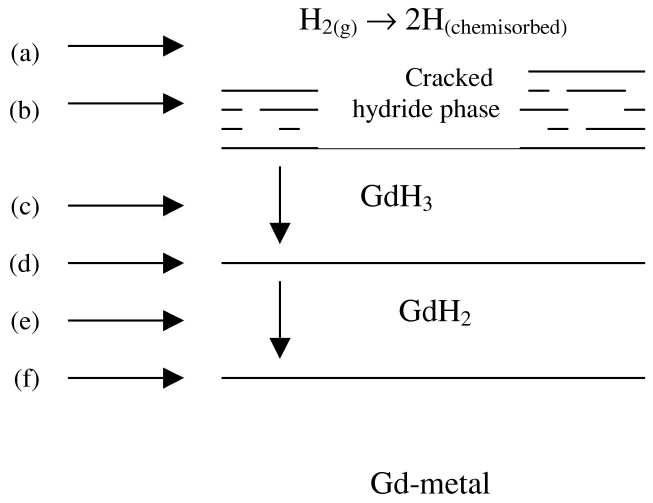

Fig. 1. A schematic structure of the hydride layer formed on top of gadolinium sample during the steady state stage of the hydriding reaction, under pressure and temperature conditions supporting the formation of the trihydride phase. The marked arrows point to the locations of possible rate determining steps: (a) adsorption (chemisorption) on the hydride; (b) surface penetration; (c) diffusion through GdH_3 phase; (d) trihydride–dihydride interface penetration; (e) diffusion through GdH_2 phase; (f) dihydride–metal interface penetration and reaction.

penetration into the subsurface of the trihydride phase, Fig. 1b, or the slow diffusion of hydrogen through the trihydride layer, Fig. 1c. It can be at the trihydride–dihydride interface, Fig. 1d, at the dihydride layer (diffusion of hydrogen through the dihydride, Fig. 1e), or at the metal–dihydride interface, Fig. 1f. The separate formation of the dihydride and trihydride phases during the hydriding reaction cannot be identified on the basis of the kinetics curve alone (except for the special cases mentioned above). More direct methods are required. Metallographic examination of cross-sections of partially hydrided rare-earth metals revealed two layers of hydride product distinguished by their different colors (yellowish outer layer and blue inner layer) [5]. The external and the inner layers were attributed to tri- and dihydride phases, respectively.

In the present work we use combined microscopic examination, X-ray diffraction (XRD), and hydrogen absorption measurements to follow the separate formation of the two hydride phases on gadolinium metallic samples.

2. Experimental

High-purity gadolinium samples (99.9%, Research Chemicals) were used for the partial hydriding experiments. The samples were discs 10 mm in diameter and 1 mm thick cut from a rod. Before the introduction into the quartz reactor, the sample discs were covered all over with evaporated gold. Then, one face of each disc was polished to 1 μm and rinsed with ethanol and water. The purpose of the gold evaporation was to prevent as much as possible hydrogen attack on the sample surface except for the examined face. Exposures were performed in conventional quartz P–V–T (Sieverts) system. The sample was vacuum annealed at 200°C for 60 min prior to exposure. Then, the sample was cooled down to 100°C and exposed to hydrogen gas under a constant pressure of 0.05 MPa (maximum pressure drop was less than 8%) and the number of hydrogen moles reacted with the sample were calculated from the pressure drop during the hydriding process. As the preset value of reaction, has been reached (which took ~5–20 min), immediate pumping of the system stopped the reaction.

The partially reacted samples were photographed using a Nikon stereoscope and the photographs were analyzed using a computer image analysis software (Image Pro) to obtain the fraction of surface area transformed into hydride phase (the hydride coverage). Right after a sample had been photographed for analysis, an XRD was measured at the attacked surface. The diffraction patterns were analyzed quantitatively using Reitveld analysis software from which, the volume fraction of each of the three phases was obtained.

Hydride powder samples were prepared for reference. Metal samples were vacuum annealed at 300°C for 30 min, then exposed to hydrogen at 0.1 MPa until the reaction was completed. The hydride was decomposed then under vacuum at 700°C and exposed again to 0.09 MPa of hydrogen. Evacuating the chamber and cooling down slowly produced a fine powder of stochiometric dihydride. The trihydride was produced by similar procedure, except that the last exposure was performed under 0.09 MPa of hydrogen at temperature of 300°C. The powder was cooled down under hydrogen to yield the GdH_3 compound for XRD. It should be mentioned that the GdH_3 powder is extremely sensitive to atmospheric oxidation. Pure silicon powder was mixed with the hydride samples for internal calibration, and the powder was encapsulated in a special sample holder to prevent oxidation.

3. Results and discussion

The reference XRD patterns of Gd metal, GdH_2, and GdH_3 are shown in Fig. 2. The diffraction patterns of the three structures are quite different; The α phase of metallic gadolinium has HCP structure, Mg-type (*$P6_3/mmc$*) [6], (a=3.636 Å, c=5.7826 Å) [7]. The GdH_2 has CaF_2 type structure (*Fm3m, cF12*) (a=5.303 Å) [8], and the GdH_3 has a HoH_3 (*P3C1*) type structure (a=6.4693 Å, c=6.7115 Å). The diffraction patterns of the pure metal and compounds were used for the Reitveld analysis which yielded the volume fraction of each of the three phases in the system.

In Fig. 3 the diffraction patterns taken from partially hydrided samples are shown together with the corresponding photomicrographs of the samples surfaces as

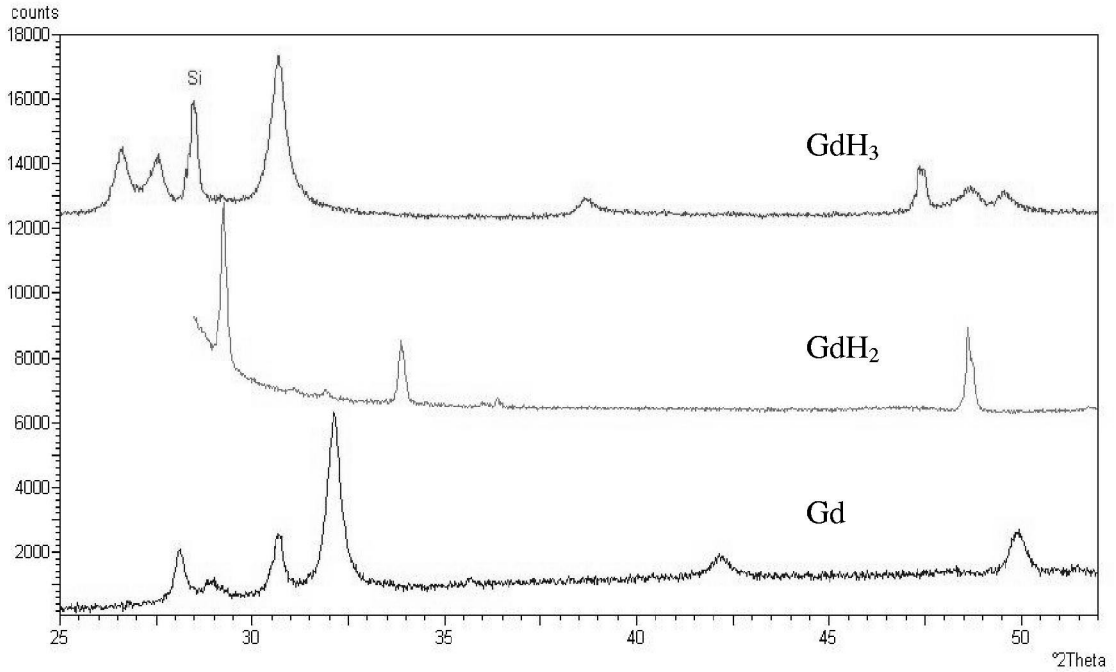

Fig. 2. X-Ray diffraction patterns of Gd, GdH_2, and GdH_3.

explained in the Experimental section. The dark parts on the micrographs represent hydride phase. The nucleation of the hydride nuclei on the metal surface is shown in Fig. 3a. The corresponding diffraction consists of a mixture of the metal and the dihydride. The hydride nuclei subsequent growth is clear in Fig. 3b and c, and the diffraction patterns point to the co-existence of all three phases, namely, the metal, the dihydride and the trihydride, on the sample surface. Eventually, the whole surface is covered with the hydride layer, as shown in Fig. 3d. At this later stage, the metal is no longer observed in the diffraction pattern, which is a mixture of the dihydride and trihydride phases. Fig. 4 represents the increase of the attacked hydrided area and the simultaneous decrease of the amount (by volume) of unreacted gadolinium metal versus the amount of absorbed hydrogen. The dependence of the fraction of gadolinium metal on the surface as a function of the absorbed hydrogen (Fig. 4a) is not linear; an initial relatively fast decrease of gadolinium on the surface is followed by almost constant value for the next stage of absorption. This means that the hydrogen absorbed at this stage has little effect on the measured amount of gadolinium metal on the surface. During hot stage microscopy measurements of the nucleation and growth of hydride phase on the surface of gadolinium metal, it was found that there is an initial nucleation stage, in which many small hydride nuclei are covering the surface below the passivation layer (the 'small-size nucleation family') [9]. This nucleation stage is followed by an incubation time in which the small nuclei stop to grow, or are growing in a very slow rate, until some of them start to grow in much faster rate to form a second class of nucleation 'family'. This behavior may account for the fast decrease and the following incubation shown in Fig. 4a.

The relation between the hydrided surface area and the amount of absorbed hydrogen is approximately linear. However, individual data points considerably deviate from the linear regression fit, as shown in Fig. 4b. There may be several reasons for this behavior: dissolution of hydrogen in the hydride phase formed as the 'small-size nucleation family' results in absorption of hydrogen with no corresponding change of the hydrided area. Also, the decrease in the rate of surface attack around 30% is probably due to the initiation of the trihydride formation, as will be shown later. For high surface attack, there are two additional error sources: first, some hydride particles spalling out from the developing nuclei may appear on the surface, being considered in mistake as additional hydrided surface. This will increase the apparent measured attacked area for a given amount of absorbed hydrogen. Second, on the other hand, increasing amounts of absorbed hydrogen are incorporated in hydride phase below the surface (hydrogen continue to penetrate into the sample after the whole surface is covered with hydrogen). This will effectively decrease the apparent measured attacked area for a given amount of absorbed hydrogen.

The changes in the relative volume percentages of the metal and hydrides on the surface are shown in Fig. 5 as a function of the hydrided attacked surface. Our main interest here is the formation of the trihydride. It is obvious that the first appearance of the trihydride phase is at relatively early stage of the hydriding reaction. The surface is only around 30% attacked when trihydride phase is starting to be observed. It should be noted that the presence

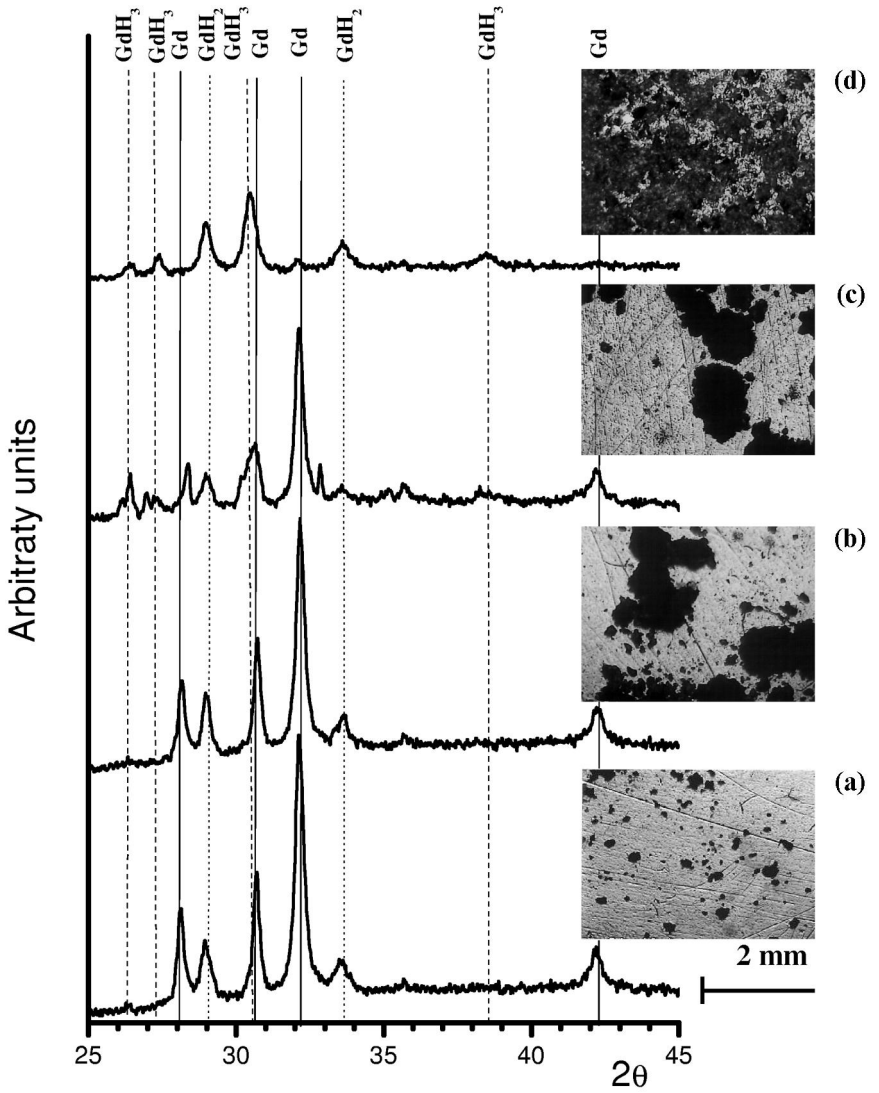

Fig. 3. X-Ray diffraction patterns and corresponding photomicrographs of partially hydrided Gd samples, vacuum annealed at 200°C for 30 min. Hydriding was performed at 100°C and under hydrogen gas pressure of 0.05 MPa. And the amount of hydrogen absorbed in the sample was: (a) 0.002 moles; (b) 0.01 moles; (c) 0.012 moles; (d) 0.016 moles.

of a new phase on the surface should be at least 5% to be observable by XRD pattern analysis. Thus, trihydride phase is formed on the sample surface during the initial growth stage of the dihydride nuclei. The decrease in the relative amount of the dihydride during the initial appearance of the trihydride phase does not reflect a real decrease in the amount of dihydride on the surface. Rather, it means that the trihydride phase appears on the dihydride phase at the gas–solid interface, masking the dihydride, which continue to grow approximately 1 μm below it (this is the analysis depth of the XRD technique). Based on these results, the topochemical development of both hydrides during the hydriding process at 100°C and under 0.5 atm of hydrogen can be deduced (1 atm=101 325 Pa). Fig. 6 displays a schematic representation of the development of both hydrides on the metallic gadolinium surface during the nucleation and growth stage of the initial hydriding reaction. At t_1 the sample is exposed to hydrogen gas. Hydrogen molecules are adsorbed and dissociate on the SPL, as described in the Introduction section. The chemisorbed hydrogen atoms then penetrate through the SPL and dissolved in the metal. When the hydrogen saturation concentration at the SPL–metal interface is exceeded, at $t_2 > t_1$ nuclei of the dihydride phase are formed under the SPL [2,3]. The dihydride nuclei are growing until at $t_3 > t_2$ nucleation of the trihydride takes place on the dihydride, at the gas–solid interface. (The SPL is ignored beyond this stage, since it is usually fractured and has no effect on the

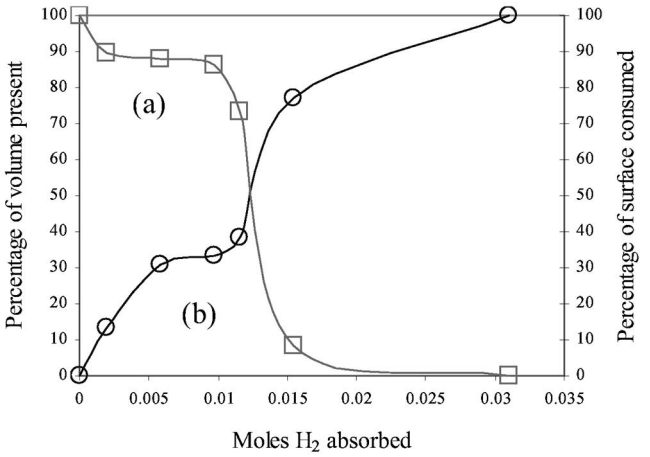

Fig. 4. (a) The decrease of the percentage (by volume) of unreacted gadolinium metal obtained from quantitative analysis of the diffraction patterns using Reitveld analysis software versus the amount of hydrogen absorbed in the sample; (b) the percentage of attacked hydrided area out of the total observed surface exposed to hydrogen. The values of the attacked surface were obtained from photomicrographs such as shown in Fig. 3 using a computer image analysis technique.

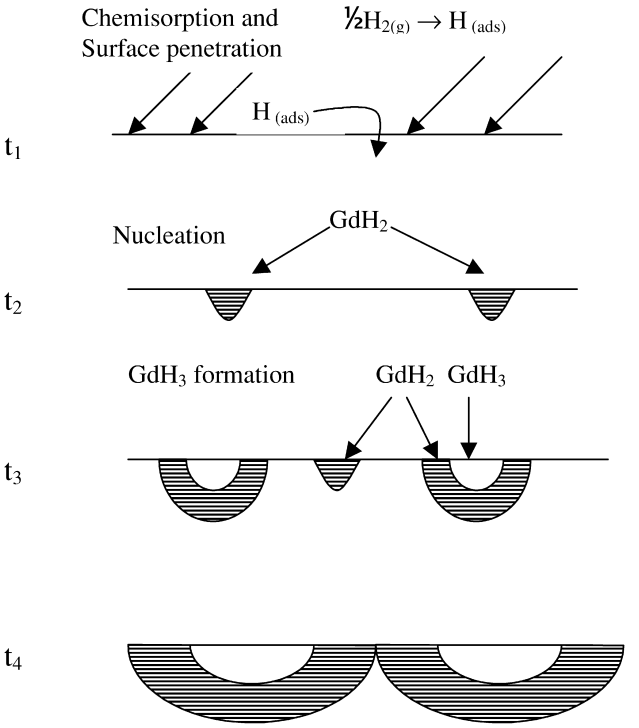

Fig. 6. A schematic representation of the development of the hydrides, GdH_2, and GdH_3, on the metallic gadolinium surface during the nucleation and growth stage of the initial hydriding reaction at 100°C and under hydrogen gas pressure of 0.05 MPa. The times $t_1<t_2<t_3<t_4$.

subsequent course of the process). It seems that the appearance of the trihydride on the surface accelerates the nucleation and growth of the dihydride as well. Notice the sharp increase in the dihydride volume percentage at 75% surface attack (Fig. 5b) and the corresponding decrease in the amount of Gd metal on the surface, Fig. 4a. Since the trihydride is located on top of the dihydride, the increase of the dihydride relative to the trihydride indicates faster growth (and nucleation) rate. However, as the hydriding reaction continues and the hydride is covering the whole sample, the relative amount of the trihydride exceeds that of the dihydride, as shown in Fig. 5.

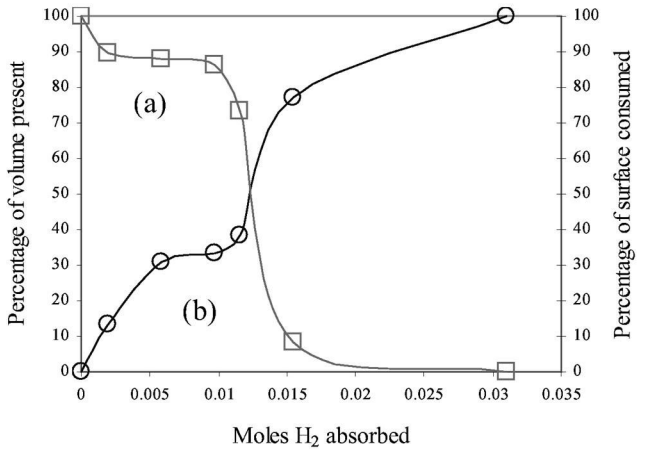

Fig. 5. Relative volume percentage of (a) metallic gadolinium; (b) the dihydride, GdH_2; and (c) the trihydride, GdH_3, for partially hydrided Gd samples, as in Fig. 3. Results were obtained from quantitative analysis of the diffraction patterns using Reitveld analysis software.

4. Conclusions

1. At 100°C and under a hydrogen gas pressure of 0.05 MPa, the hydriding reaction of gadolinium metal starts with nucleation and growth of the dihydride phase on the sample surface.
2. The trihydride is formed on top of the dihydride growing nuclei at a relatively early stage, so that when the hydride layer formation on the sample is completed, it is already constructed according to the scheme shown Fig. 1.
3. The steady state stage of the hydride layer advance during the hydriding reaction is expected to start rather early, since when the hydride layer formation on the sample is completed, it is already constructed according to the scheme shown in Fig. 1.
4. The rate-limiting step cannot be the adsorption (chemisorption) of the hydrogen gas on the dihydride. In such a case, the concentration of hydrogen on the dihydride would be low during the hydriding reaction (since the removal of hydrogen from the surface is

relatively fast in such a case). The high concentration needed for the formation of the trihydride could not be achieved until the completion of the metal to dihydride phase transformation.

Acknowledgements

This work was supported by a joint grant from the Israel Council for Higher Education and the Israel Atomic Energy Commission.

References

[1] M. Mueller, J.P. Blackledge, G.G. Libowitz, Metal Hydrides, Academic Press, New York, London, 1968.
[2] J. Bloch, M.H. Mintz, J. Alloys Comp. 253–254 (1997) 529–541.
[3] K.H. Gayer, W.G. Bos, J. Phys. Chem. 68 (1964) 2569.
[4] M.H. Mintz, J. Bloch, Prog. Solid State Chem. 16 (1985) 163–194.
[5] J. Bloch, Z. Hadari, M.H. Mintz, J. Less-Common Met. 102 (1984) 311–328.
[6] W.B. Pearson, Handbook of Lattice Spacing and Structures of Metals and Alloys, Vol. 2, Bergamon, 1967.
[7] F.H. Spedding, A.H. Daane, K.W. Herrmann, Acta Crystallogr. 9 (1956) 559.
[8] M. Ellner, H. Reule, E.J. Mittemeijer, J. Alloys Comp. 279 (1998) 179.
[9] M. Brill, J. Bloch, M.H. Mintz, to be published.